Biochemical and Biophysical Research Communications 434 (2013) 328–333

Contents lists available at SciVerse ScienceDirect

Biochemical and Biophysical Research Communications

journal homepage: www.elsevier.com/locate/ybbrc

Interaction of the S100A6 mutant (C3S) with the V domain of the receptor for advanced glycation end products (RAGE)

Sepuru K. Mohan [1], Arun A. Gupta [1], Chin Yu *

Department of Chemistry, National Tsing Hua University, Hsinchu, Taiwan

ARTICLE INFO

Article history:
Received 20 February 2013
Available online 26 March 2013

Keywords:
Receptor for advanced glycation end products (RAGE)
S100A6 (C3S)
NMR
ITC
HSQC
HADDOCK

ABSTRACT

S100A6 is involved in several vital biological functions, such as calcium sensing and cell proliferation. It is a homodimeric protein that belongs to the S100 protein family. The receptor for advanced glycation end products (RAGE) has been shown to play a role in the progression of various disease conditions, such as diabetes and immune/inflammatory disorders. Information regarding the association of RAGE with S100 proteins at a molecular level is useful to understand the diversity of the RAGE signaling pathways. In this report, biomolecular NMR techniques were utilized for the resonance assignment of the C3S mutation in human S100A6 and characterizing its interaction with the RAGE V domain. Further binding affinity between S100A6m and the RAGE V domain was determined by isothermal titration calorimetric studies. HADDOCK was used to generate a heterotetramer model of the S100A6m–RAGE V domain complex. This model provides an important insights into the S100–RAGE cellular signaling pathway.

1. Introduction

S100A6 is a 10.2 kDa homodimeric protein that belongs to the S100 subfamily of Ca^{2+}-binding proteins. S100A6 can be considered as the best representative of the S100 protein family due to its typical EF hand sequence, and biological function as a calcium signal transmitter [1]. S100A6 was named calcyclin for its calcium affinity and its role in the progression of various cancers which have been identified in different tissues [2]. S100A6 is prominently a cytoplasmic protein, but its presence has been observed in extracellular physiological fluid [3].

RAGE is a cell surface receptor that binds to multifarious ligands with diverse structural features, such as S100 proteins, glycated proteins, amyloid-β and HMGB1 [4,5]. RAGE signaling plays a central role in chronic inflammatory disorders [6] and certain cancers [7]. RAGE is now widely known as a universal extracellular receptor for S100 proteins, thus mediating their biological effects [8]. The signaling pathways activated upon the binding of extracellular S100A6 with the RAGE receptor have been studied recently [9].

The solved X-ray calcium bound structure of human S100A6 [10] and the holo form of the NMR structure of rabbit S100A6 [11] have been published previously. Based on the amino acid sequence alignment, we observed that there is only 88% homology between the rabbit and human form of S100A6. Thus, we embarked upon the sequential assignment of a calcium bound human mutation (C3S) of S100A6 (S100A6m), to explore the various facets of S100A6m interaction with the RAGE V domain. Our results demonstrate that S100A6m interacts with the RAGE V domain in a symmetrical fashion forming a heterotetrameric complex.

2. Materials and methods

2.1. Expression and purification of S100A6m and RAGE V domain

Human S100A6 contains a single cysteine residue, making the presence of DTT as a reducing agent in NMR buffer conditions necessary. To study the interaction with the RAGE V domain, cysteine-3 was mutated to a serine in the human S100A6 sequence, because the structural stability of RAGE V domain is dramatically altered in the presence of the reducing agent. The recombinant S100A6m protein was over expressed in *Escherichia coli* BL21(DE3) strain using the pET-20b(+) T7 expression vector. The purification of S100A6m was achieved using the previously described protocol [12]. The samples used for NMR spectroscopy contained 1.0–1.5 mM ^{13}C, ^{15}N-labeled or ^{15}N-labeled S100A6m.

The RAGE V domain protein was overexpressed in the pET-15b(+) expression vector using BL21(DE3) CodonPlus as host cells. The initial purification steps were followed as described previously [13]. The final purification of the N-terminal His tag cleaved sample was performed on a C-18 HPLC column (Atlantis). The RAGE V protein was eluted as a single fraction from HPLC, which was

* Corresponding author. Address: Department of Chemistry, National Tsing Hua University, No. 101, Section 2, Kuang-Fu Road, Hsinchu 30013, Taiwan. Fax: +886 35 711082.

E-mail addresses: mohansepuri@gmail.com (S.K. Mohan), ninja14gupta@gmail.com (A.A. Gupta), cyu.nthu@gmail.com (C. Yu).

[1] These authors contributed equally to this work.

0006-291X/$ - see front matter © 2013 Elsevier Inc. All rights reserved.
http://dx.doi.org/10.1016/j.bbrc.2013.03.049

lyophillised and stored at −20 °C for further use. The purity of both of the purified protein samples was estimated to be ~95% by SDS–PAGE and, HPLC, and the molecular weight was confirmed using ESI-TOF mass spectrometry.

2.2. NMR resonance assignments

All NMR experiments were performed at 298 K on a Varian Inova 700 MHz spectrometer equipped with a cold probe head with a sample concentration for S100A6m in the range of 1–1.5 mM. The samples were prepared in 20 mM Tris-d_6 (pH 7.0, in 90% H_2O and 10% D_2O) containing 10 mM $CaCl_2$ and, 0.01% sodium azide. The sequence specific assignments of polypeptide backbone for S100A6m were made from the ^1H–^{15}N HSQC, HNCO [14], HNCA [15], HN(CO)CA [16], HNCACB [17] and CBCA(CO)NH [18] spectra. The backbone dihedral angles were predicted using the TALOS + software [19]. The NMR data were processed using VNMRJ 2.3 and analyzed using Sparky [20].

2.3. Isothermal titration calorimetry

The protein–protein interactions were demonstrated by measuring the heat change during the titration of its partner protein ligand into the protein solution using a Microcal iTC200 Calorimeter [21]. The overnight dialyzed S100A6m and RAGE V domain protein samples in 50 mM Tris HCl (pH 7.0) containing 10 mM $CaCl_2$ were centrifuged and degassed under vacuum before use. The titrations were performed at (25 °C) by injecting 2 μL aliquots of 1 mM RAGE V domain as the protein ligand (20 injections) into 0.1 mM of the S100A6m solution over a period of 6 s separated by 240 s for further injections. The results of the experimental protein–protein titration curve were corrected using protein-buffer control experiment, further analyzed and fitted to a single site binding model using Origin 7.0 software supplied by Microcal.

2.4. ^1H–^{15}N HSQC titration

For the ^1H–^{15}N HSQC titration experiments, the concentration of the proteins used was ~0.2 mM. The ^1H–^{15}N HSQC titrations were performed in 50 mM Tris–HCl (in 90% H_2O:10% D_2O), with 10 mM calcium chloride buffer conditions at pH ~7.0. For the first set of experiments, ^{15}N-labeled S100A6m (0.15 mM) protein was incrementally titrated with unlabeled RAGE V domain (1.5 mM) protein up to 1:1 molar ratio to form the protein complex. The reciprocal titrations were conducted using the incremental addition of unlabeled S100A6m (2 mM) protein to ^{15}N-labeled RAGE V domain (0.2 mM) to form a 1:1 protein complex.

2.5. Size exclusion chromatography

Analytical size exclusion chromatography was performed at room temperature on Superdex75 column attached to the AKTA FPLC system (GE). The column was equilibrated with 50 mM Tris–HCl (pH 7.0) and 10 mM $CaCl_2$ containing buffer, with flow rate of 0.5 ml/min. The column was pre-calibrated using the following protein standards (GE): bovine serum albumin (67 kDa), chicken ovalbumin (44 kDa), chymotrypsin (26 kDa), and ribonuclease (13 kDa) [22].

2.6. Docking studies

HADDOCK [23,24] was used to dock S100A6 and the RAGE V domain in the tetrameric complex. For the multi-body docking studies, human S100A6 (PDB ID:1K9K) and the RAGE V domain (PDB ID:2E5E) coordinates were taken from the Protein Data Bank as input data. The chemical shift perturbed residues were used to define the ambiguous interaction restraints (AIR) as the intermolecular constraints for the docking protocol. Active residues and passive residues were defined as those having both chemical shift perturbations and a relative residue accessible surface area larger and smaller than 50% for either side-chain or backbone atoms, respectively, as calculated by NACCESS [25] (Supplementary Fig. 3A). The calculated complex structure ensemble were further analyzed using PROCHECK [26].

3. Results and discussion

3.1. Assignments

The ^1H–^{15}N HSQC spectra of S100A6m is well dispersed and 84 cross peaks in the HSQC spectrum have been assigned unambiguously (Supplementary Fig. 1A). The back bone ^1H–^{15}N resonances of Met 1, Pro 4, Ile 9, His 17, Lys 32 and Ala 54 could not be assigned. Regions near these sites exhibited weak NMR signals in all spectra collected. The ^1H, ^{13}C and ^{15}N chemical shifts for human S100A6m have been deposited in the BioMagResBank under the BMRB accession number 18854.

The wild type S100A6 protein form in all reported species is known to have a single cysteine residue. The only notable exception is the rabbit form with a serine at this position [2]. The cysteine residue in wild type human S100A6 is located in an unstructured region of protein (PDB ID:1K9K). We drew HSQC spectrum comparisons between the wild type and mutated

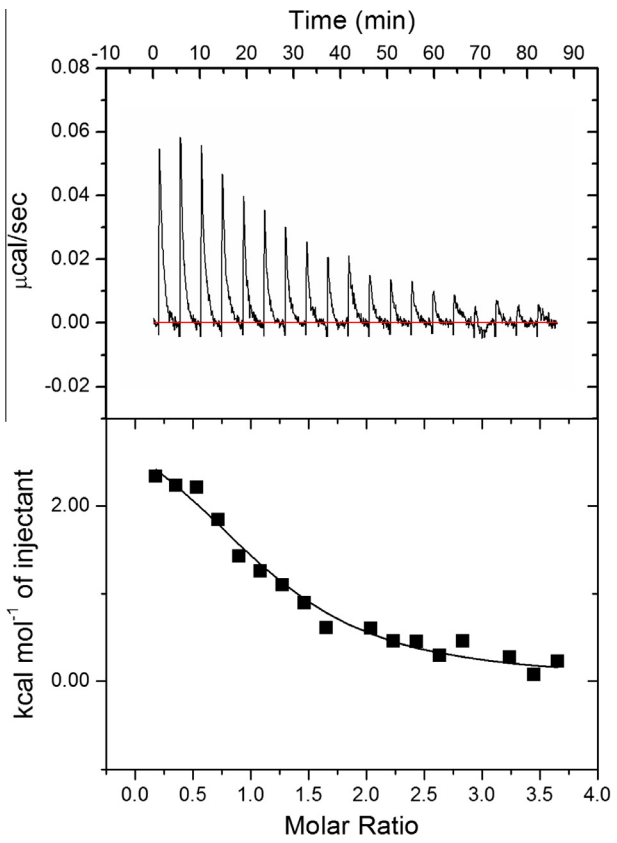

Fig. 1. An isothermogram representing the binding of RAGE V domain to the S100A6m at 25 °C. The binding constant characterizing the S100A6m–RAGE V domain interaction was 3.00 μM. The upper panels show the raw titration data, and the lower panels show the integrated heat changes after subtracting the heat of dilution. The titrations were performed in 50 mM Tris (pH 7.0) containing 10 mM $CaCl_2$. The concentration of RAGE V domain and the S100A6m used in the ITC experiments were 1.0 and 0.1 mM, respectively.

S100A6 C3S form (Supplementary Fig. 1B), which suggested that the mutated S100A6 (C3S) structure would be similar to the wild type structure as reported in the Protein Data Bank (PDB ID:1K9K) [10]. This observation further suggests, that a serine mutation at position 3 will not have any overall effect on the tertiary structure of the human S100A6 protein, with potential implications related only to the detrimental effect in formation of higher order oligomers [2].

3.2. Binding thermodynamics

The isothermogram in Fig. 1 represents the binding between RAGE V domain and S100A6m with a binding affinity (K_d) of 3.00 μM. Further analysis of the fitted ITC isothermogram for single site model revealed the stoichiometry of the S100A6m–RAGE V domain interaction was (1:1), symbolizing the symmetrical binding interface of two molecules of the RAGE V domain for one dimer of S100A6m. Positive values for the enthalpy (ΔH = 3.35 kcal/mol) and entropy (ΔS = 33.6 cal/mol/degree) suggests the interaction between the two proteins was more likely to be an entropically driven process. This observation further implies the role of buried apolar surface residues in the near vicinity or on the interface of the S100A6m–RAGE V domain complex. Our findings are relevant in the context of previously reported results for S100B–RAGE complex [27].

3.3. Size exclusion chromatography

Analytical size exclusion chromatography is a useful technique to describe changes in the molecular size of a free protein that is complexed upon protein–protein interaction. The free S100A6m and free RAGE V domain eluted as single peaks at 14.0 and 15.5 ml, respectively. The extrapolation of this elution volume on the standard plot (log molecular weight versus elution volume) yields a molecular size of 22.0 and 12.0 kDa, respectively. The isolated single peak from the size exclusion column at 11.7 ml for an equivalent 1:1 protein sample mixture of the RAGE V domain and S100A6m was reinjected to the size exclusion column to confirm

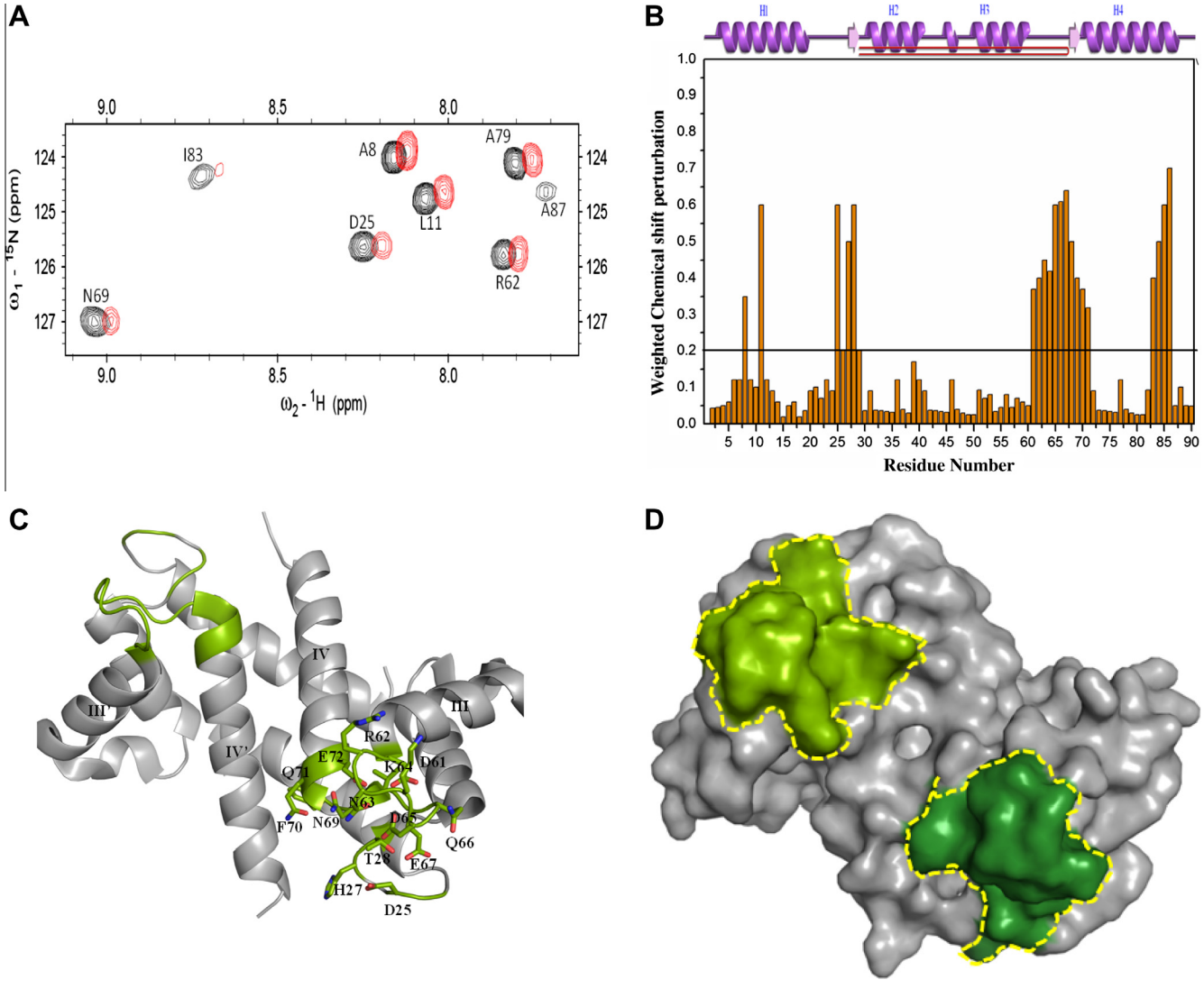

Fig. 2. Analysis of S100A6m (^{15}N labeled)–RAGE V domain complex using 2D NMR at a 1:1 binding ratio. (A) The overlaid 2D [^{1}H–^{15}N]-HSQC spectra highlight the spectral changes of the uniformly ^{15}N-labeled free S100A6m (black) and S100A6m upon binding to RAGE V-domain (red). (B) The weighted average of the chemical shift (^{1}H and ^{15}N) perturbations $\{\Delta\delta = [(\delta^1\mathrm{HN})^2 + 0.2\,(\delta^{15}\mathrm{N})^2]^{1/2}\}$ of the amino acid residues in S100A6m upon complex formation with the RAGE V domain are represented as a bar graph. (C) Cartoon representation of the S100A6m dimer with the perturbed side chain residues side chain displayed light green. (D) The surface representation of S100A6m dimer with perturbed residues painted as symmetrical patches on one molecule as light green and other molecule as dark green. (For interpretation of the references to colour in this figure legend, the reader is referred to the web version of this article.)

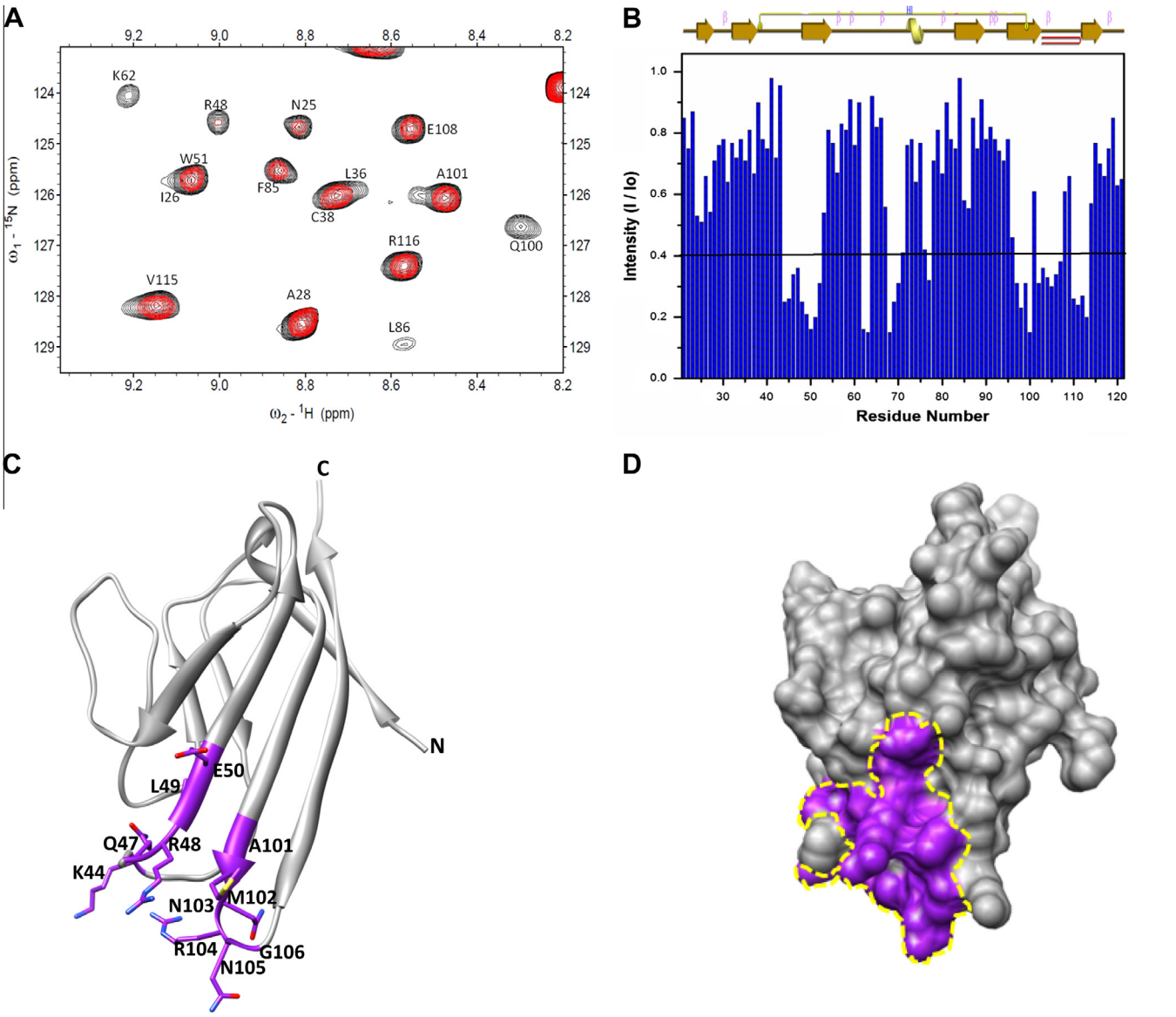

Fig. 3. Analysis of the S100A6m–RAGE V domain (^{15}N labeled) complex using 2D NMR at a 1:1 binding ratio. (A) The overlaid 2D [^{1}H–^{15}N]-HSQC spectra highlights the intensity changes in the uniformly ^{15}N-labeled free RAGE V (black) and RAGE V domain upon binding to S100A6m (red). (B) The cross peak intensity plot of (I/I_o) where (I) is S100A6m–RAGE V domain complex intensity and (I_o) is the initial intensity of free RAGE V protein versus the residue number are represented as a bar. (C) A cartoon representation of the RAGE V domain with residues showing dropped intensities labeled in magenta. (D) The surface representation of the RAGE V domain with residues in which the intensity dropped shown in magenta depicting one full surface for S100A6 interaction. (For interpretation of the references to colour in this figure legend, the reader is referred to the web version of this article.)

the molecular size of the protein–protein complex corresponding to 43.0 kDa. This elution profile clearly represents the S100A6m–RAGE V domain tetrameric complex (Supplementary Fig. 2A).

3.4. Mapping the binding interface

Evaluating ^{1}H–^{15}N chemical shift perturbations in the ^{1}H–^{15}N HSQC spectrum provides residue-level information for mapping the protein–protein interface between the two protein partners [28]. The ^{1}H–^{15}N HSQC spectra of free S100A6m and free RAGE V domain are well-dispersed. The assignment of RAGE V domain was derived from already deposited BMRB data (Accession number 7364) as reported in literature [29] and also confirmed by NMR backbone experiments (Supplementary Fig. 2B). At a S100A6m (^{15}N labeled):RAGE V domain (unlabeled) titration ratio of 1:1, we observed that some cross peaks were significantly perturbed upon complex formation, whereas the chemical shifts of the other residues are similar to those of free S100A6m, suggesting a fast exchange regime for S100A6m:RAGE V domain titration (Fig. 2A). Further plotted analysis of the chemical shift perturbed residues (Fig. 2B), revealed that most of the altered residues on S100A6m upon complexation with the RAGE V domain were predominantly distributed over loop 1, loop 3 and helix 4 (Fig. 2C and D). The reciprocal HSQC experiments in which S100A6m (unlabeled) was titrated to RAGE V domain (^{15}N labeled) at a formed complex ratio of 1:1, showed a differential change in cross peak intensities for some residues in RAGE V domain HSQC spectrum, characteristic of the intermediate exchange (Fig. 3A). Analysis of the change in cross peak intensity plot of the intensity dropped residues, provided the specific information regarding residues that are likely to constitute the S100A6m binding site(s) on the RAGE V domain (Fig. 3B). We portrayed those residues for which the intensity

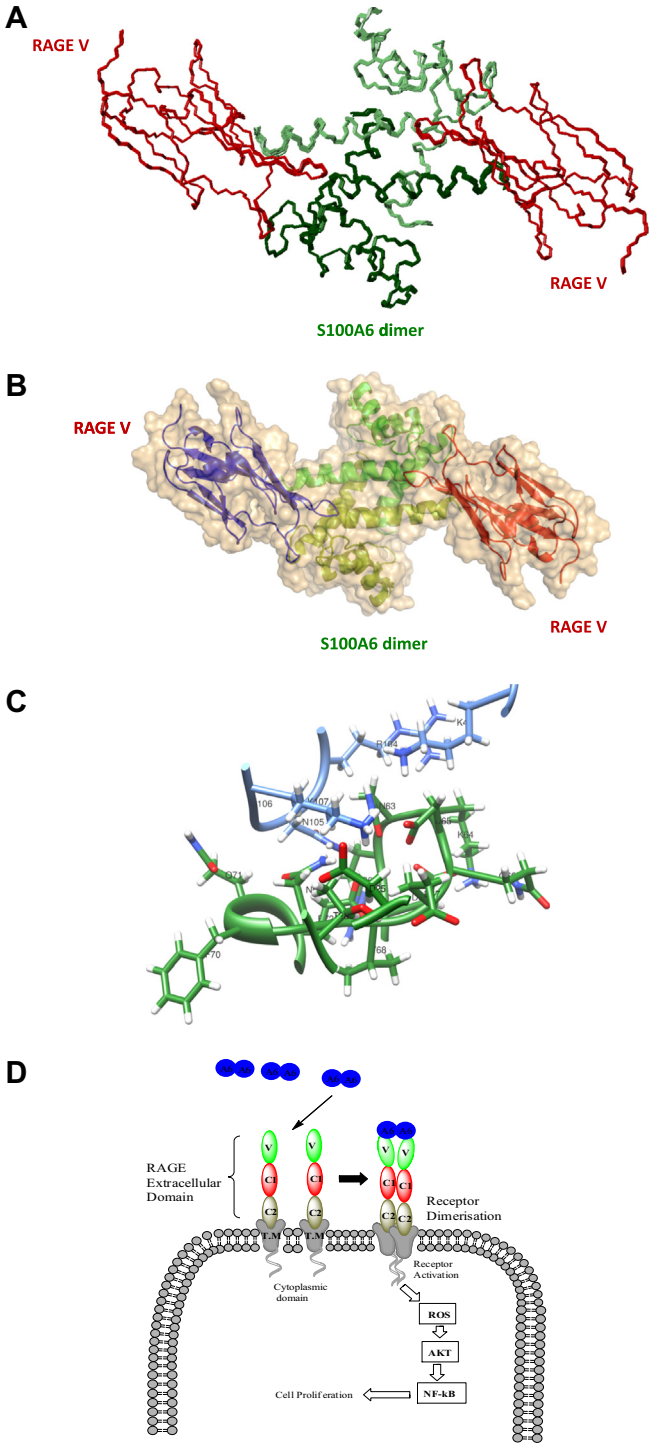

Fig. 4. HADDOCK results and the S100A6–RAGE V domain signaling pathway (A) a representation of ensemble of 10 structures of S100A6–RAGE V complex (B) the surface representation of Haddock calculated model of the S100A6–RAGE V domain heterotetrameric complex, with the secondary structure elements of S100A6 homodimer shown in dark green and lemon. The RAGE V domain molecules and the secondary structure elements are shown in red and blue respectively. (C) A close view of the side chain of the interface residues represented as ball stick model in green for S100A6 and blue for the RAGE V domain. (D) The proposed mechanism of S100A6–RAGE V domain signaling pathway with S100A6 dimer binds with RAGE V domain. Then the cytoplasmic domain of the two receptors associate triggering generation of the reactive oxygen species (ROS), which will induce Akt kinase activation, leading to the downstream initiation of NF-kB, causing further cell proliferation. (For interpretation of the references to colour in this figure legend, the reader is referred to the web version of this article.)

dropped significantly on the RAGE V domain structure (Fig. 3C) to decipher the S100A6m binding region which was spread over the N-terminal beta strands, beta turns and C-terminal beta hairpin motifs (Fig. 3D).

3.5. Structure of S100A6m–RAGE V domain complex

A total of 4000 rigid-body docking trials were conducted using the standard HADDOCK protocol, with 200 structures used for subsequent semi-flexible simulated annealing and final refinement in explicit water as a solvent layer. HADDOCK clustered 194 structures in five clusters. Out of the five clusters generated, Cluster 1 comprised of 104 structures with a pairwise lowest RMSD value of 0.6 Å when compared to 9.3 Å RMSD for second most populated Cluster 2 with 71 structures (Supplementary Fig. 3B). The higher RMSD score value implied poor geometry for the Cluster 2 structures from the lowest energy conformation. Owing to its lesser buried surface area of 2026 $\mathbf{Å^2}$ and higher HADDOCK score value of −137 for Cluster 2, it was also evident to select Cluster 1 for further analysis (Supplementary Fig. 3C). The structural properties of the 10 lowest energy structures (Fig. 4A) from this cluster were further validated with PROCHECK (Supplementary Fig. 4A) and deposited as an ensemble in the Protein Data Bank under the entry code 2M1K. The surface representation of the S100A6m–RAGE V domain tetrameric complex (shown in Fig. 4B).

3.6. S100A6m–RAGE V domain interface

The differential binding specificities within the various S100 proteins of the S100 family suggest a versatile manner in which each S100 proteins recognize an array of partner proteins [30–32]. The identified hot spots on the RAGE V domain surface for S100A6m interaction consisted mainly of basic charged residues like Lys-44, Arg-48, Arg-98, Arg-104 and Lys-107. The notable residues on the RAGE V binding interface included Met-102 and Gly-106 which constituted the hydrophobic patch that interacts with S100A6m. Other residues, including Gln-47, Leu-49, Glu-50, Gln-100, Asn-103 and Asn-105, provided the contacts to interact with S100A6m and were in the vicinity of the basic residues to define one contiguous surface on the RAGE V domain (Fig. 4C). It is important to mention here that some of the basic charged residues on the RAGE V domain involved in the S100A6m–RAGE V domain interaction are also conserved in the AGE–RAGE interaction and the S100B–RAGE VC1 model complex [29,33]. The residues on S100A6, that were distributed on the interfacial region of the protein–protein complex included Gly-24, Thr-28, Arg-62, Asn-63, Lys-64, Gln-66, Asn-69 and Phe-70. The surface complementary acidic residues that described the crucial binding recognition face for the RAGE V domain interaction on S100A6m are Asp-25, Asp-65 and Glu-67. This interfacial information led us to identify unique structural features, which differentiate the interaction of S100A6 for RAGE V domain, were mapped to non-conserved residues on 2nd EF hand and loop 1 of S100A6, in contrast to sequentially diverse hinge region of S100B which plays the key role in RAGE VC1 interaction (Supplementary Fig. 4B) [33]. Overall, we imply that calcium bound S100A6 will facilitate the interaction between S100A6 and its protein partners.

3.7. The mechanism of S100A6 signaling to RAGE

Oligomerisation of the extracellular domains is known to occur in the immunoglobulin family of receptor proteins for cellular signaling. The dimerization of the RAGE receptor is an important step for receptor activation during ligand binding [33,34]. The RAGE V domain has been proposed to associate on cell surface to promote ligand binding [35]. In our present work, the homodimer of human

S100A6 interacts with two extracellular RAGE V domains forming a tetrameric complex. This complex formation will cause further association and autophosphorylation between the cytoplasmic domains resulting in the initiation of downstream secondary cellular messengers, thus giving evidence in favor of role of RAGE V domain in RAGE dimerisation for signal transduction (Fig. 4D) [13]. Further the distinction can be made for S100A6–RAGE V domain complex from the previous reports [13,33], as this interaction signifies the role of dimeric form S100A6 [32] having symmetrical binding interface with RAGE V domain compared to higher order oligomeric form of S100B associating with RAGE V domain. These conclusions will add impetus to the current literature, signifying the importance of S100A6 induced cell proliferation on RAGE receptor activation, triggered by generation of reactive oxygen species (ROS) which further involve activation of PI 3-kinase/AKT and NF-kB transcription factor [9]. These findings provide a better understanding of the role of S100A6 in RAGE signaling, thus helping to develop future therapeutic strategies to ameliorate RAGE related diseases [36].

Acknowledgment

We would like to acknowledge the financial support from the National Science Council (NSC) of Taiwan (Grant number NSC 100-2113-M-007-012-MY3).

Appendix A. Supplementary data

Supplementary data associated with this article can be found, in the online version, at http://dx.doi.org/10.1016/j.bbrc.2013.03.049.

References

[1] E. Leclerc, G. Fritz, S.W. Vetter, C.W. Heizmann, Binding of S100 proteins to RAGE: an update, Biochimica et Biophysica Acta (BBA) – Molecular Cell Research 1793 (2009) 993–1007.
[2] W. Leśniak, Ł.P. Słomnicki, A. Filipek, S100A6 – new facts and features, Biochemical and Biophysical Research Communications 390 (2009) 1087–1092.
[3] G. Thordarson, J.N. Southard, F. Talamantes, Purification and characterization of mouse decidual calcyclin: a novel stimulator of mouse placental lactogen-II secretion, Endocrinology 129 (1991) 1257–1265.
[4] S. Yan, R. Ramasamy, A. Schmidt, Receptor for AGE (RAGE) and its ligands – cast into leading roles in diabetes and the inflammatory response, Journal of Molecular Medicine 87 (2009) 235–247.
[5] A. Bierhaus, P. Humpert, M. Morcos, T. Wendt, T. Chavakis, B. Arnold, D. Stern, P. Nawroth, Understanding RAGE, the receptor for advanced glycation end products, Journal of Molecular Medicine 83 (2005) 876–886.
[6] M.A. Hofmann, S. Drury, C. Fu, W. Qu, A. Taguchi, Y. Lu, C. Avila, N. Kambham, A. Bierhaus, P. Nawroth, M.F. Neurath, T. Slattery, D. Beach, J. McClary, M. Nagashima, J. Morser, D. Stern, A.M. Schmidt, RAGE mediates a novel proinflammatory axis: a central cell surface receptor for S100/calgranulin polypeptides, Cell 97 (1999) 889–901.
[7] A. Taguchi, D.C. Blood, G. del Toro, A. Canet, D.C. Lee, W. Qu, N. Tanji, Y. Lu, E. Lalla, C. Fu, M.A. Hofmann, T. Kislinger, M. Ingram, A. Lu, H. Tanaka, O. Hori, S. Ogawa, D.M. Stern, A.M. Schmidt, Blockade of RAGE–amphoterin signalling suppresses tumour growth and metastases, Nature 405 (2000) 354–360.
[8] R. Donato, RAGE: a single receptor for several ligands and different cellular responses: the case of certain S100 proteins, Current Molecular Medicine 7 (2007) 711–724.
[9] E. Leclerc, G. Fritz, M. Weibel, C.W. Heizmann, A. Galichet, S100B and S100A6 differentially modulate cell survival by interacting with distinct RAGE (receptor for advanced glycation end products) immunoglobulin domains, Journal of Biological Chemistry 282 (2007) 31317–31331.
[10] L.R. Otterbein, J. Kordowska, C. Witte-Hoffmann, C.L.A. Wang, R. Dominguez, Crystal structures of S100A6 in the Ca^{2+}-free and Ca^{2+}-bound states: the calcium sensor mechanism of S100 proteins revealed at atomic resolution, Structure (London, England) 10 (2002) (1993) 557–567.
[11] M. Sastry, R.R. Ketchem, O. Crescenzi, C. Weber, M.J. Lubienski, H. Hidaka, W.J. Chazin, The three-dimensional structure of Ca^{2+}-bound calcyclin: implications for Ca^{2+}-signal transduction by S100 proteins, Structure 6 (1998) 223–231.
[12] A. Gupta, S. Mohan, Y. Chin, ^{1}H, ^{13}C and ^{15}N backbone and side chain resonance assignments of human halo S100A1, Biomolecular NMR Assignments 6 (2012) 213–215.
[13] B.M. Dattilo, G. Fritz, E. Leclerc, C.W. Vander Kooi, C.W. Heizmann, W.J. Chazin, The extracellular region of the receptor for advanced glycation end products is composed of two independent structural units†, Biochemistry 46 (2007) 6957–6970.
[14] D.R. Muhandiram, L.E. Kay, Gradient-enhanced triple-resonance three-dimensional NMR experiments with improved sensitivity, Journal of Magnetic Resonance, Series B 103 (1994) 203–216.
[15] M. Ikura, L.E. Kay, A. Bax, A novel approach for sequential assignment of proton, carbon-13, and nitrogen-15 spectra of larger proteins: heteronuclear triple-resonance three-dimensional NMR spectroscopy. Application to calmodulin, Biochemistry 29 (1990) 4659–4667.
[16] A. Bax, M. Ikura, An efficient 3D NMR technique for correlating the proton and ^{15}N backbone amide resonances with the α-carbon of the preceding residue in uniformly $^{15}N/^{13}C$ enriched proteins, Journal of Biomolecular NMR 1 (1991) 99–104.
[17] M. Wittekind, L. Mueller, HNCACB, a high-sensitivity 3D NMR experiment to correlate amide–proton and nitrogen resonances with the alpha- and beta-carbon resonances in proteins, Journal of Magnetic Resonance, Series B 101 (1993) 201–205.
[18] S. Grzesiek, A. Bax, Correlating backbone amide and side chain resonances in larger proteins by multiple relayed triple resonance NMR, Journal of the American Chemical Society 114 (1992) 6291–6293.
[19] Y. Shen, F. Delaglio, G. Cornilescu, A. Bax, TALOS+: a hybrid method for predicting protein backbone torsion angles from NMR chemical shifts, Journal of Biomolecular NMR 44 (2009) 213–223.
[20] T.D. Goddard, D.G. Kneller, SPARKY 3, University of California, San Francisco, 2002.
[21] M.M. Pierce, C.S. Raman, B.T. Nall, Isothermal titration calorimetry of protein–protein interactions, Methods 19 (1999) 213–221.
[22] P. Andrews, B.T. Nall, Estimation of the molecular weight of proteins by Sephadex gel filtration, The Biochemical Journal 91 (1964) 222–233.
[23] C. Dominguez, R. Boelens, A.M.J.J. Bonvin, HADDOCK: a protein−protein docking approach based on biochemical or biophysical information, Journal of the American Chemical Society 125 (2003) 1731–1737.
[24] S.J. de Vries, M. van Dijk, A.M.J.J. Bonvin, The HADDOCK web server for data-driven biomolecular docking, Nat. Protocols 5 (2010) 883–897.
[25] S.J. Hubbard, J.M. Thornton, 'NACCESS', Computer Program, Department of Biochemistry and Molecular Biology, University College London, 1993.
[26] R. Laskowski, J.A. Rullmann, M. MacArthur, R. Kaptein, J. Thornton, AQUA and PROCHECK-NMR: programs for checking the quality of protein structures solved by NMR, Journal of Biomolecular NMR 8 (1996) 477–486.
[27] H. Park, J.C. Boyington, The 1.5 Å crystal structure of human receptor for advanced glycation endproducts (RAGE) ectodomains reveals unique features determining ligand binding, Journal of Biological Chemistry 285 (2010) 40762–40770.
[28] D.S. Garrett, Y.-J. Seok, A. Peterkofsky, G.M. Clore, A.M. Gronenborn, Identification by NMR of the binding surface for the histidine-containing phosphocarrier protein HPr on the N-terminal domain of enzyme I of the *Escherichia coli* phosphotransferase system†, Biochemistry 36 (1997) 4393–4398.
[29] S. Matsumoto, T. Yoshida, H. Murata, S. Harada, N. Fujita, S. Nakamura, Y. Yamamoto, T. Watanabe, H. Yonekura, H. Yamamoto, T. Ohkubo, Y. Kobayashi, Solution structure of the variable-type domain of the receptor for advanced glycation end products: new insight into AGE−RAGE interaction†,‡, Biochemistry 47 (2008) 12299–12311.
[30] S. Bhattacharya, C.G. Bunick, W.J. Chazin, Target selectivity in EF-hand calcium binding proteins, Biochimica et Biophysica Acta (BBA) – Molecular Cell Research 1742 (2004) 69–79.
[31] A. Rezvanpour, G.S. Shaw, Unique S100 target protein interactions, General Physiology and Biophysics 28 (2009) F39–F65.
[32] Y.-T. Lee, Y.N. Dimitrova, G. Schneider, W.B. Ridenour, S. Bhattacharya, S.E. Soss, R.M. Caprioli, A. Filipek, W.J. Chazin, Structure of the S100A6 complex with a fragment from the C-terminal domain of siah-1 interacting protein: a novel mode for S100 protein target recognition†‡, Biochemistry 47 (2008) 10921–10932.
[33] M. Koch, S. Chitayat, B.M. Dattilo, A. Schiefner, J. Diez, W.J. Chazin, G. Fritz, Structural basis for ligand recognition and activation of RAGE, Structure 18 (2010) 1342–1352.
[34] J. Xie, S. Reverdatto, A. Frolov, R. Hoffmann, D.S. Burz, A. Shekhtman, Structural basis for pattern recognition by the receptor for advanced glycation end products (RAGE), Journal of Biological Chemistry 283 (2008) 27255–27269.
[35] Z. Sárkány, T.P. Ikonen, F. Ferreira-da-Silva, M.J. Saraiva, D. Svergun, A.M. Damas, Solution structure of the soluble receptor for advanced glycation end products (SRAGE), Journal of Biological Chemistry 286 (2011) 37525–37534.
[36] S.F. Yan, R. Ramasamy, A.M. Schmidt, Soluble RAGE: therapy and biomarker in unraveling the RAGE axis in chronic disease and aging, Biochemical Pharmacology 79 (2010) 1379–1386.